DIFFUSION LANGUAGE MODELS KNOW THE ANSWER BEFORE DECODING

Pengxiang Li[1], Yefan Zhou[2], Dilxat Muhtar[6,7], Lu Yin[3], Shilin Yan, Li Shen[4], Yi Liang[5]
Soroush Vosoughi[2], Shiwei Liu[6,7]
[1]The Hong Kong Polytechnic University   [2]Dartmouth College   [3]University of Surrey   [4]Sun Yat-sen University
[5]Google DeepMind   [6]Max Planck Institute for Intelligent Systems   [7]ELLIS Institute Tübingen

ABSTRACT

Diffusion language models (DLMs) have recently emerged as an alternative to autoregressive approaches, offering parallel sequence generation and flexible token orders. However, their inference remains slower than that of autoregressive models, primarily due to the cost of bidirectional attention and the large number of refinement steps required for high-quality outputs. In this work, we highlight and leverage an overlooked property of DLMs—**early answer convergence**: in many cases, the correct answer can be internally identified by half steps before the final decoding step, both under semi-autoregressive and random re-masking schedules. For example, on GSM8K and MMLU, up to 97% and 99% of instances, respectively, can be decoded correctly using only half of the refinement steps. Building on this observation, we introduce **Prophet**, a training-free fast decoding paradigm that enables **early commit decoding**. Specifically, Prophet dynamically decides whether to continue refinement or to go "all-in" (i.e., decode all remaining tokens in one step), using the confidence gap between the top-2 prediction candidates as the criterion. It integrates seamlessly into existing DLM implementations, incurs negligible overhead, and requires no additional training. Empirical evaluations of LLaDA-8B and Dream-7B across multiple tasks show that Prophet reduces the number of decoding steps by up to 3.4× while preserving high generation quality. These results recast DLM decoding as a problem of *when to stop sampling*, and demonstrate that early decode convergence provides a simple yet powerful mechanism for accelerating DLM inference, complementary to existing speedup techniques. Our code is available at `https://github.com/pixeli99/Prophet`.

1 INTRODUCTION

Along with the rapid evolution of diffusion models in various domains (Ho et al., 2020; Nichol & Dhariwal, 2021; Ramesh et al., 2021; Saharia et al., 2022; Jing et al., 2022), Diffusion language models (DLMs) have emerged as a compelling and competitively efficient alternative to autoregressive (AR) models for sequence generation (Austin et al., 2021a; Lou et al., 2023; Shi et al., 2024; Sahoo et al., 2024; Nie et al., 2025; Gong et al., 2024; Ye et al., 2025). Primary strengths of DLMs over AR models include, but are not limited to, efficient parallel decoding and flexible generation orders. More specifically, DLMs decode all tokens in parallel through iterative denoising and re-masking steps. The remaining tokens are typically refined with low-confidence predictions over successive rounds (Nie et al., 2025).

Despite the speed-up potential of DLMs, the inference speed of DLMs is slower than AR models in practice, due to the lack of KV-cache mechanisms and the significant performance degradation associated with fast parallel decoding (Israel et al., 2025a). Recent endeavors have proposed excellent algorithms to enable KV-cache (Ma et al., 2025a; Liu et al., 2025a; Wu et al., 2025a) and improve the performance of parallel decoding (Wu et al., 2025a; Wei et al., 2025a; Hu et al., 2025).

In this paper, we aim to accelerate the inference of DLMs from a different perspective, motivated by an overlooked yet powerful phenomenon of DLMs—**early answer convergence**. Through extensive analysis, we observed that: *a strikingly high proportion of samples can be correctly decoded during*

the early phase of decoding for both semi-autoregressive remasking and random remasking. This trend becomes more significant for random remasking. For example, on GSM8K and MMLU, up to 97% and 99% of instances, respectively, can be decoded correctly using only half of the refinement steps.

Motivated by this finding, we introduce **Prophet**, a training-free fast decoding strategy designed to capitalize on early answer convergence. Prophet continuously monitors the confidence gap between the top-2 answer candidates throughout the decoding trajectory, and opportunistically decides whether it is safe to decode all remaining tokens at once. By doing so, Prophet achieves substantial inference speed-up (up to 3.4×) while maintaining high generation quality. Our contributions are threefold:

- **Empirical observations of early answer convergence:** We demonstrate that a strikingly high proportion of samples (up to 99%) can be correctly decoded during the early phase of decoding for both semi-autoregressive remasking and random remasking. This underscores a fundamental redundancy in conventional full-length slow decoding.

- **A fast decoding paradigm enabling early commit decoding:** We propose Prophet, which evaluates at each step whether the remaining answer is accurate enough to be finalized immediately, which we call Early Commit Decoding. We find that the confidence gap between the top-2 answer candidates serves as an effective metric to determine the right time of early commit decoding. Leveraging this metric, Prophet dynamically decides between continued refinement and immediate answer emission.

- **Substantial speed-up gains with high-quality generation:** Experiments across diverse benchmarks reveal that Prophet delivers up to 3.4× reduction in decoding steps. Crucially, this acceleration incurs negligible degradation in accuracy-affirming that early commit decoding is not just computationally efficient but also semantically reliable for DLMs.

2 RELATED WORK

2.1 DIFFUSION LARGE LANGUAGE MODEL

The idea of adapting diffusion processes to discrete domains traces back to the pioneering works of Sohl-Dickstein et al. (2015); Hoogeboom et al. (2021). A general probabilistic framework was later developed in D3PM (Austin et al., 2021a), which modeled the forward process as a discrete-state Markov chain progressively adding noise to the clean input sequence over time steps. The reverse process is parameterized to predict the clean text sequence based on the current noisy input by maximizing the Evidence Lower Bound (ELBO). This perspective was subsequently extended to the continuous-time setting. Campbell et al. (2022) reinterpreted the discrete chain within a continuous-time Markov chain (CTMC) formulation. An alternative line of work, SEDD (Lou et al., 2023), focused on directly estimating likelihood ratios and introduced a denoising score entropy criterion for training. Recent analyses in MDLM (Shi et al., 2024; Sahoo et al., 2024; Zheng et al., 2024) and RADD (Ou et al., 2024) demonstrate that multiple parameterizations of MDMs are in fact equivalent.

Motivated by these groundbreaking breakthroughs, practitioners have successfully built product-level DLMs. Notable examples include commercial releases such as Mercury (Labs et al., 2025), Gemini Diffusion (DeepMind, 2025), and Seed Diffusion (Song et al., 2025b), as well as open-source implementations including LLaDA (Nie et al., 2025) and Dream (Ye et al., 2025). However, DLMs face an efficiency-accuracy tradeoff that limits their practical advantages. While DLMs can theoretically decode multiple tokens per denoising step, increasing the number of simultaneously decoded tokens results in degraded quality. Conversely, decoding a limited number of tokens per denoising step leads to high inference latency compared to AR models, as DLMs cannot naively leverage key-value (KV) caching or other advanced optimization techniques due to their bidirectional nature.

2.2 ACCELERATION METHODS FOR DIFFUSION LANGUAGE MODELS

To enhance the inference speed of DLMs while maintaining quality, recent optimization efforts can be broadly categorized into three complementary directions. One strategy leverages the empirical

observation that hidden states exhibit high similarity across consecutive denoising steps, enabling approximate caching (Ma et al., 2025b; Liu et al., 2025b; Hu et al., 2025). The alternative strategy restructures the denoising process in a semi-autoregressive or block-autoregressive manner, allowing the system to cache states from previous context or blocks. These methods may optionally incorporate cache refreshing that update stored cache at regular intervals (Wu et al., 2025b; Arriola et al., 2025; Wang et al., 2025b; Song et al., 2025a). The second direction reduces attention cost by pruning redundant tokens. For example, DPad (Chen et al., 2025) is a training-free method that treats future (suffix) tokens as a computational "scratchpad" and prunes distant ones before computation. The third direction focuses on optimizing sampling methods or reducing the total denoising steps through reinforcement learning (Song et al., 2025b). Sampling optimization methods aim to increase the number of tokens decoded at each denoising step through different selection strategies. These approaches employ various statistical measures—such as confidence scores or entropy—as thresholds for determining the number of tokens to decode simultaneously. The token count can also be dynamically adjusted based on denoising dynamics (Wei et al., 2025b; Huang & Tang, 2025), through alignment with small off-the-shelf AR models (Israel et al., 2025b) or use the DLM itself as a draft model for speculative decoding (Agrawal et al., 2025).

Different from the above optimization methods, our approach stems from the observation that DLMs can correctly predict the final answer at intermediate steps, enabling early commit decoding to reduce inference time. Note that the early answer convergence has also been discovered by an excellent concurrent work (Wang et al., 2025a), where they focus on averaging predictions across time steps for improved accuracy, whereas we develop an early commit decoding method that reduces computational steps while maintaining quality.

3 PRELIMINARY

3.1 BACKGROUND ON DIFFUSION LANGUAGE MODELS

Concretely, let $x_0 \sim p_{\text{data}}(x_0)$ be a clean input sequence. At an intermediate noise level $t \in [0, T]$, we denote by x_t the corrupted version obtained after applying a masking procedure to a subset of its tokens.

Forward process. The corruption mechanism can be expressed as a Markov chain

$$q(x_{1:T} \mid x_0) = \prod_{t=1}^{T} q(x_t \mid x_{t-1}), \tag{1}$$

which gradually transforms the original sample x_0 into a maximally degraded representation x_T. At each step, additional noise is injected, so that the sequence becomes progressively more masked as t increases.

While the forward process in Eq.(1) is straightforward, its exact reversal is typically inefficient because it unmasks only one position per step (Campbell et al., 2022; Lou et al., 2023). To accelerate generation, a common remedy is to use the τ-*leaping* approximation (Gillespie, 2001), which enables multiple masked positions to be recovered simultaneously. Concretely, transitioning from corruption level t to an earlier level $s < t$ can be approximated as

$$q_{s|t} = \prod_{i=1}^{n} q_{s|t}(x_s^i \mid x_t), \quad q_{s|t}(x_s^i \mid x_t) = \begin{cases} 1, & x_t^i \neq [\text{MASK}], \ x_s^i = x_t^i, \\ \frac{s}{t}, & x_t^i = [\text{MASK}], \ x_s^i = [\text{MASK}], \\ \frac{t-s}{t} \, q_{0|t}(x_s^i \mid x_t), & x_t^i = [\text{MASK}], \ x_s^i \neq [\text{MASK}]. \end{cases} \tag{2}$$

Here, $q_{0|t}(x_s^i \mid x_t)$ is a predictive distribution over the vocabulary, supplied by the model itself, whenever a masked location is to be unmasked. In conditional generation (e.g., producing a response x_0 given a prompt p), this predictive distribution additionally depends on p, i.e., $q_{0|t}(x_s^i \mid x_t, p)$.

Reverse generation. To synthesize text, one needs to approximate the reverse dynamics. The generative model is parameterized as

$$p_\theta(x_{0:T}) = p_\theta(x_T) \prod_{t=1}^{T} p_\theta(x_{t-1} \mid x_t) = \prod_{t=1}^{T} q(x_{t-1} \mid x_0) \, p_\theta(x_0 \mid x_t). \tag{3}$$

This reverse process naturally decomposes into two complementary components. **i. Prediction step.** The model $p_\theta(x_0 \mid x_t)$ attempts to reconstruct a clean sequence from the corrupted input at level t. We denote the predicted sequence after this step by x_0^t, i.e. $x_0^t = p_\theta(x_0 \mid x_t)$. (2) **ii. Re-masking step.** Once a candidate reconstruction x_0^t is obtained, the forward noising mechanism is reapplied in order to produce a partially corrupted sequence x_{t-1} that is less noisy than x_t. This "re-masking" can be implemented in various ways, such as masking tokens uniformly at random or selectively masking low-confidence positions (Nie et al., 2025). Through the interplay of these two steps—prediction and re-masking—the model iteratively refines an initially noisy sequence into a coherent text output.

3.2 EARLY ANSWER CONVERGENCY

In this section, we investigate the early emergence of correct answers in DLMs. We conduct a comprehensive analysis using LLaDA-8B (Nie et al., 2025) on two widely used benchmarks: GSM8K (Cobbe et al., 2021) and MMLU (Hendrycks et al., 2021). Specifically, we examine the decoding dynamics, that is, how the top 1 predicted token evolves across positions at each decoding step, and report the percentage of the full decoding process at which the top 1 predicted tokens first match the ground truth answer tokens. In this study, we only consider samples where the final output contains the ground truth answer.

For low confidence remasking, we set Answer length at 256 and Block length at 32 for GSM8K, and Answer length at 128 and Block length to 128 for MMLU. For random remasking, we set Answer length at 256 and Block length at 256 for GSM8K, and Answer length at 128 and Block length at 128 for MMLU.
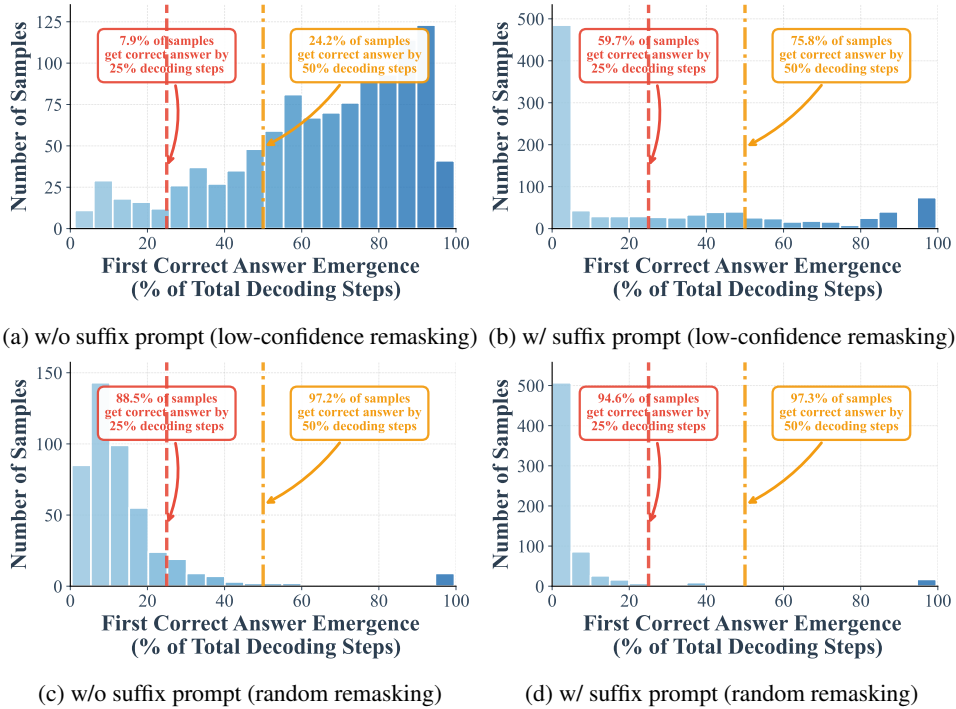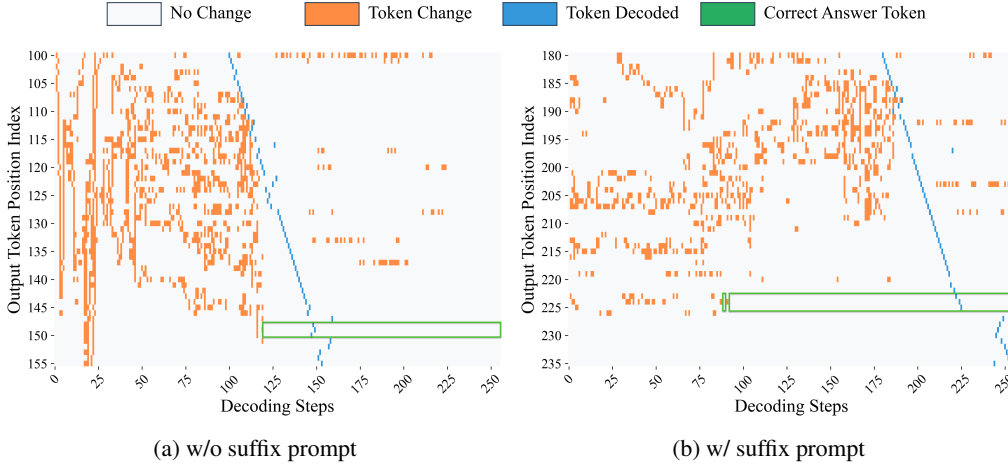

(a) w/o suffix prompt (low-confidence remasking) (b) w/ suffix prompt (low-confidence remasking)

(c) w/o suffix prompt (random remasking) (d) w/ suffix prompt (random remasking)

Figure 1: **Distribution of early correct answer detection during decoding process.**. Histograms show when correct answers first emerge during diffusion decoding, measured as percentage of total decoding steps, using `LLaDA 8B` on `GSM8K`. Red and orange dashed lines indicate 50% and 70% completion thresholds, with corresponding statistics showing substantial early convergence. Suffix prompting (b,d) dramatically accelerates convergence compared to standard prompting (a,c). This early convergence pattern demonstrates that correct answer tokens stabilize as top-1 candidates well before full decoding.

4

I. A high proportion of samples can be correctly decoded during the early phase of decoding. Figure 1(a) demonstrates that when remasking with the low-confidence strategy, 24.2% samples are already correctly predicted in the first half steps, and 7.9% samples can be correctly decoded in the first 25% steps. These two numbers will be further largely boosted to 97.2% and 88.5%, when shifted to random remasking as shown in Figure 1-(c).

II. Our suffix prompt further amplifies the early emergence of correct answers. Adding the suffix prompt "Answer:" significantly improves early decoding. With low confidence remasking, the proportion of correct samples emerging by the 25% step rises from 7.9% to 59.7%, and by the 50% step from 24.2% to 75.8% (Figure 1-(b)). Similarly, under random remasking, the 25% step proportion increases from 88.5% to 94.6%.

III. Decoding dynamics of chain-of-thought tokens. We further examine the decoding dynamics of chain-of-thought tokens in addition to answer tokens, as shown in Figure 2. First, most non-answer tokens fluctuate frequently before being finalized. Second, answer tokens change far less often and tend to stabilize earlier, remaining unchanged for the rest of the decoding process.

Figure 2: **Decoding dynamics across all positions based on maximum-probability predictions.** Heatmaps track how the top-1 token changes at each position, if it is decoded at the current step, over the course of decoding. (a) Without our suffix prompts, correct answer tokens reach maximum probability at step 119. (b) With our suffix prompts, this occurs earlier at step 88, showing that the model internally identifies correct answers well before the final output. Results are shown for `LLaDA 8B` solving problem index 700 from GSM8K under low-confidence decoding. Gray indicates positions where the top-1 prediction remains unchanged, orange marks positions where the prediction changes to a different token, blue denotes the step at which the corresponding y-axis position is actually decoded, and green box highlights the answer region where the correct answer remains stable as the top-1 token and can be safely decoded without further changes as the decoding process progresses.

4 METHODOLOGY

Built upon the above findings, we introduce **Prophet**, a training-free fast decoding algorithm designed to accelerate the generation phase of DLMs. Prophet by committing to all remaining tokens in one shot and predicting answers as soon as the model's predictions have stabilized, which we call Early Commit Decoding. Unlike conventional fixed-step decoding, Prophet actively monitors the model's certainty at each step to make an informed, on-the-fly decision about when to finalize the generation.

Confidence Gap as a Convergence Metric. The core mechanism of Prophet is the **Confidence Gap**, a simple yet effective metric for quantifying the model's conviction for a given token. At any decoding step t, the DLM produces a logit matrix $\mathbf{L}_t \in \mathbb{R}^{N \times |\mathcal{V}|}$, where N is the sequence length
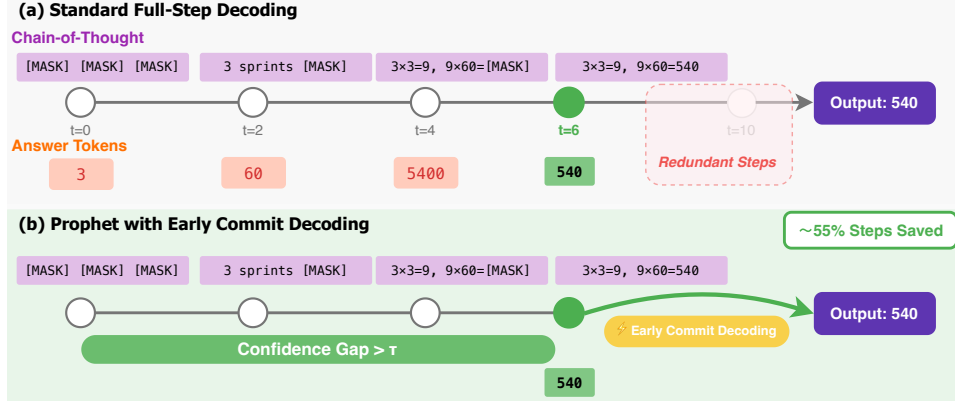
Figure 3: An illustration of the Prophet's early-commit-decoding mechanism. **(a)** Standard full-step decoding completes all predefined steps (e.g., 10 steps), incurring redundant computations after the answer has stabilized (at t=6). **(b)** Prophet dynamically monitors the model's confidence (the "Confidence Gap"). It triggers an early commit decoding as soon as the answer converges, saving a significant portion of the decoding steps (in this case, 55%) without compromising the output quality.

and $|\mathcal{V}|$ is the vocabulary size. For each position i, we identify the highest logit value, $L_{t,i}^{(1)}$, and the second-highest, $L_{t,i}^{(2)}$. The confidence gap $g_{t,i}$ is defined as their difference:

$$g_{t,i} = L_{t,i}^{(1)} - L_{t,i}^{(2)}. \tag{4}$$

This value serves as a robust indicator of predictive certainty. A large probability gap signals that the prediction has likely converged, with the top-ranked token clearly outweighing all others.

Early Commit Decoding. The decision of when to terminate the decoding loop can be framed as an optimal stopping problem. At each step, we must balance two competing costs: the **computational cost** of performing additional refinement iterations versus the **risk of error** from a premature and potentially incorrect decision. The computational cost is a function of the remaining steps, while the risk of error is inversely correlated with the model's predictive certainty, for which the Confidence Gap serves as a robust proxy.

Prophet addresses this trade-off with an adaptive strategy that embodies a principle of **time-varying risk aversion**. Let denote $p = (T_{\max} - t)/T_{\max}$ as the decoding progress, where $T_{\max}$ is the total number of decoding steps, and $\tau(p)$ is the threshold for early commit decoding. In the early, noisy stages of decoding (when progress p is small), the potential for significant prediction improvement is high. Committing to an answer at this stage carries a high risk. Therefore, Prophet acts in a risk-averse manner, demanding an exceptionally high threshold (τ_{high}) to justify an early commit decoding, ensuring such a decision is unequivocally safe. As the decoding process matures (as p increases), two things happen: the model's predictions stabilize, and the potential computational savings from stopping early diminish. Consequently, the cost of performing one more step becomes negligible compared to the benefit of finalizing the answer. Prophet thus becomes more risk-tolerant, requiring a progressively smaller threshold (τ_{low}) to confirm convergence.

This dynamic risk-aversion policy is instantiated through our staged threshold function, which maps the abstract trade-off between inference speed and generation certainty onto a concrete decision rule:

$$\bar{g}_t \geq \tau(p), \quad \text{where} \quad \tau(p) = \begin{cases} \tau_{\text{high}} & \text{if } p < 0.33 \\ \tau_{\text{mid}} & \text{if } 0.33 \leq p < 0.67 \\ \tau_{\text{low}} & \text{if } p \geq 0.67 \end{cases} \tag{5}$$

Once the exit condition is satisfied at step t^*, the iterative loop is terminated. The final output is then constructed in a single parallel operation by filling any remaining [MASK] tokens with the argmax of the current logits $\mathbf{L}_{t^*}$.

Algorithm Summary. The complete Prophet decoding procedure is outlined in Algorithm 1. The integration of the confidence gap check adds negligible computational overhead to the standard DLM

decoding loop. Prophet is model-agnostic, requires no retraining, and can be readily implemented as a wrapper around existing DLM inference code.

Algorithm 1 Prophet: Early Commit Decoding for Diffusion Language Models

---

1: **Input:** Model M_θ, prompt $\mathbf{x}_{\text{prompt}}$, max steps $T_{\max}$, generation length N_{gen}
2: **Input:** Threshold function $\tau(\cdot)$, answer region positions $\mathcal{A}$
3: Initialize sequence $\mathbf{x}_T \leftarrow \text{concat}(\mathbf{x}_{\text{prompt}}, [\text{MASK}]^{N_{\text{gen}}})$
4: Let $\mathcal{M}_t$ be the set of masked positions at step t.
5: **for** $t = T_{\max}, T_{\max} - 1, \ldots, 1$ **do**
6:     Compute logits: $\mathbf{L}_t = M_\theta(\mathbf{x}_t)$
7:                                       ▷ **Prophet's Early-Commit-Decoding Check**
8:     Calculate average confidence gap $\bar{g}_t$ over positions $\mathcal{A}$ using Eq. 4.
9:     Calculate progress: $p \leftarrow (T_{\max} - t)/T_{\max}$
10:     **if** $\bar{g}_t \geq \tau(p)$ **then**   ▷ Check condition from Eq. 5
11:         $\hat{\mathbf{x}}_0 \leftarrow \text{argmax}(\mathbf{L}_t, \dim = -1)$
12:         $\mathbf{x}_0 \leftarrow \mathbf{x}_t$. Fill positions in $\mathcal{M}_t$ with tokens from $\hat{\mathbf{x}}_0$.
13:         **Return** $\mathbf{x}_0$ ▷ Terminate and finalize
14:     **end if**
15:                                     ▷ **Standard DLM Refinement Step**
16:     Determine tokens to unmask $\mathcal{U}_t \subseteq \mathcal{M}_t$ via a re-masking strategy.
17:     $\hat{\mathbf{x}}_0 \leftarrow \text{argmax}(\mathbf{L}_t, \dim = -1)$
18:     Update $\mathbf{x}_{t-1} \leftarrow \mathbf{x}_t$, replacing tokens at positions $\mathcal{U}_t$ with those from $\hat{\mathbf{x}}_0$.
19: **end for**
20: **Return** $\mathbf{x}_0$ ▷ Return result after full iterations if no early commit decoding

---

5 EXPERIMENTS

We evaluate Prophet on diffusion language models (DLMs) to validate two key hypotheses: first, that Prophet can preserve the performance of full-budget decoding while using substantially fewer denoising steps; second, that our adaptive approach provides more reliable acceleration than naive static baselines. We demonstrate that Prophet achieves notable computational savings with negligible quality degradation through comprehensive experiments across diverse benchmarks.

5.1 EXPERIMENTAL SETUP

We conduct experiments on two state-of-the-art diffusion language models: LLaDA-8B (Nie et al., 2025) and Dream-7B (Ye et al., 2025). For each model, we compare three decoding strategies: **Full** uses the standard diffusion decoding with the complete step budget of $T_{\max}$ and **Prophet** employs early commit decoding with dynamic threshold scheduling. The threshold parameters are set to $\tau_{\text{high}} = 7.5$, $\tau_{\text{mid}} = 5.0$, and $\tau_{\text{low}} = 2.5$, with transitions occurring at 33% and 67% of the decoding progress. These hyperparameters were selected through preliminary validation experiments.

Our evaluation spans four capability domains to comprehensively assess Prophet's effectiveness. For general reasoning, we use MMLU (Hendrycks et al., 2021), ARC-Challenge (Clark et al., 2018), HellaSwag (Zellers et al., 2019), TruthfulQA (Lin et al., 2021), WinoGrande (Sakaguchi et al., 2021), and PIQA (Bisk et al., 2020). Mathematical and scientific reasoning are evaluated through GSM8K (Cobbe et al., 2021) and GPQA (Rein et al., 2023). For code generation, we employ HumanEval (Chen et al., 2021) and MBPP (Austin et al., 2021b). Finally, planning capabilities are assessed using Countdown and Sudoku tasks (Gong et al., 2024). We follow the prompt in simple-evals for LLaDA and Dream, making the model reason step by step. Concretely, we set the generation length L to 128 for general tasks, to 256 for GSM8K and GPQA, and to 512 for the code benchmarks. Unless otherwise noted, all baselines use a number of iterative steps equal to the specified generation length. All experiments employ greedy decoding to ensure deterministic and reproducible results.

Table 1: Benchmark results on LLaDA-8B-Instruct and Dream-7B-Instruct. Sudoku and Countdown are evaluated using 8-shot setting; all other benchmarks use zero-shot evaluation. Detailed configuration is listed in the Appendix.

Benchmark	LLaDA 8B	LLaDA 8B (Ours)	Gain (Δ)	Dream-7B	Dream-7B (Ours)	Gain (Δ)
		General Tasks				
MMLU	54.1	54.0 (2.34×)	-0.1	67.6	66.1 (2.47×)	-1.5
ARC-C	83.2	83.5 (1.88×)	+0.3	88.1	87.9 (2.61×)	-0.2
Hellaswag	68.7	70.9 (2.14×)	+2.2	81.2	81.9 (2.55×)	+0.7
TruthfulQA	34.4	46.1 (2.31×)	+11.7	55.6	53.2 (1.83×)	-2.4
WinoGrande	73.8	70.5 (1.71×)	-3.3	62.5	62.0 (1.45×)	-0.5
PIQA	80.9	81.9 (1.98×)	+1.0	86.1	86.6 (2.29×)	+0.5
		Mathematics & Scientific				
GSM8K	77.1	77.9 (1.63×)	+0.8	75.3	75.2 (1.71×)	-0.1
GPQA	25.2	25.7 (1.82×)	+0.5	27.0	26.6 (1.66×)	-0.4
		Code				
HumanEval	30.5	30.5 (1.20×)	0.0	54.9	55.5 (1.44×)	+0.6
MBPP	37.6	37.4 (1.35×)	-0.2	54.0	54.6 (1.33×)	+0.6
		Planning Tasks				
Countdown	15.3	15.3 (2.67×)	0.0	14.6	14.6 (2.37×)	0.0
Sudoku	35.0	38.0 (2.46×)	+3.0	89.0	89.0 (3.40×)	0.0

5.2 MAIN RESULTS AND ANALYSIS

The results of our experiments are summarized in Table 1. Across the general reasoning tasks, Prophet demonstrates its ability to match or even exceed the performance of the full baseline. For example, using LLaDA-8B, Prophet achieves 54.0% on MMLU and 83.5% on ARC-C, both of which are statistically on par with the full step decoding. Interestingly, on HellaSwag, Prophet (70.9%) not only improves upon the full baseline (68.7%) but also the half baseline (70.5%), suggesting that early commit decoding can prevent the model from corrupting an already correct prediction in later, noisy refinement steps. Similarly, Dream-7B maintains competitive performance across benchmarks, with Prophet achieving 66.1% on MMLU compared to the full model's 67.6%—a minimal drop of 1.5% while delivering 2.47× speedup.

Prophet continues to prove its reliability in more complex reasoning tasks, including mathematics, science, and code generation. For the GSM8K dataset, Prophet with LLaDA-8B obtains an accuracy of 77.9%, outperforming the baseline's 77.1%. This reliability also extends to code generation benchmarks. For instance, on HumanEval, Prophet perfectly matches the full baseline's score with LLaDA-8B (30.5%) and even slightly improves it with Dream-7B (55.5% vs. 54.9%). Notably, the acceleration on these intricate tasks (e.g., 1.20× on HumanEval) is more conservative compared to general reasoning. This demonstrates Prophet's adaptive nature: it dynamically allocates more denoising steps when a task demands further refinement, thereby preserving accuracy on complex problems. This reinforces Prophet's role as a "safe" acceleration method that avoids the pitfalls of premature, static termination.

In summary, our empirical results strongly support the central hypothesis of this work: DLMs often determine the correct answer long before the final decoding step. Prophet successfully capitalizes on this phenomenon by dynamically monitoring the model's predictive confidence. It terminates the iterative refinement process as soon as the answer has stabilized, thereby achieving significant computational savings with negligible, and in some cases even positive, impact on task performance. This stands in stark contrast to static truncation methods, which risk cutting off the decoding process prematurely and harming accuracy. Prophet thus provides a robust and model-agnostic solution to accelerate DLM inference, enhancing its practicality for real-world deployment.

5.3 ABLATION STUDIES

Beyond the coarse step–budget ablation above, we further dissect why Prophet outperforms static truncation by examining (i) sensitivity to the generation length L and available step budget, (ii) robustness to the granularity of semi-autoregressive block updates, and (iii) compatibility with differ-

Table 2: **GSM8K ablations**. (a) Accuracy vs. step budget under two generation lengths L. Prophet stops early (average steps in parentheses) yet matches/exceeds the full-budget baseline. (b) Accuracy under different re-masking strategies; Prophet complements token-selection policies.

(a) Accuracy vs. step budget and generation length

L	16	32	64	128	Prophet (avg. steps; speedup)	Full
256	7.7	22.5	58.8	76.2	**77.9** ($\approx$160; 1.63$\times$)	77.1
128	21.8	50.3	67.9	71.3	**72.7** ($\approx$74; 1.73$\times$)	71.3

(b) Re-masking strategy

Strategy	Baseline	Ours (Prophet)
Random	63.8	**66.6**
Low-confidence	71.3	**72.7**
Top-k margin	72.4	**73.1**

Table 3: **Sensitivity to block length** on GSM8K (semi-autoregressive updates). Prophet is less brittle to coarse-grained updates and yields larger gains as block length increases.

Block length	8	16	32	64	128
Baseline	67.1	68.7	71.3	59.9	33.1
Ours (Prophet)	**72.8**	**73.3**	**72.7**	**69.8**	**52.2**
Δ (Abs.)	+5.7	+4.6	+1.4	+9.9	+19.1

ent re-masking heuristics. Together, these studies consistently show that Prophet's adaptive early-commit rule improves the compute–quality Pareto frontier, whereas static schedules either under-compute (hurting accuracy) or over-compute (wasting steps).

Accuracy vs. step budget under different L. Table 2 (Panel A) summarizes GSM8K accuracy as we vary the number of refinement steps under two generation lengths ($L = 256$ and $L = 128$). Accuracy under a static step cap rises monotonically with more steps (e.g., $7.7\% \to 22.5\% \to 58.8\% \to 76.2\%$ for 16/32/64/128 at $L = 256$), but still underperforms either the full-budget decoding or Prophet. In contrast, Prophet stops adaptively at ≈ 160 steps for $L = 256$ (saving $\approx 38\%$ steps; $256/160 \approx 1.63\times$) and yields a higher score than the 256-step baseline (77.9% vs. 77.1%). When the target length is shorter ($L = 128$), Prophet again surpasses the 128-step baseline (72.7% vs. 71.3%) while using only ≈ 74 steps (saving $\approx 42\%$; $128/74 \approx 1.73\times$). These results reaffirm that the gains are not a byproduct of simply using fewer steps: Prophet avoids late-stage over-refinement when the answer has already stabilized, while still allocating extra iterations when needed.

Granularity of semi-autoregressive refinement (block length). Table 3 shows that static block schedules are brittle: accuracy peaks around moderate blocks and collapses for large blocks (e.g., 59.9 at 64 and 33.1 at 128). Prophet markedly attenuates this brittleness, delivering consistent gains across the entire range, and especially at large blocks where over-aggressive parallel updates inject more noise. For instance, at block length 64 and 128, Prophet improves accuracy by $+9.9$ and $+19.1$ points, respectively. This robustness is a direct consequence of Prophet's time-varying risk-aversion: when coarse-grained updates raise uncertainty, the threshold schedule defers early commit; once predictions settle, Prophet exits promptly to avoid additional noisy revisions.

Re-masking strategy compatibility. Table 2 (Panel B) evaluates three off-the-shelf re-masking heuristics (random, low-confidence, top-k margin). Prophet consistently outperforms their static counterparts, with the largest gain under random re-masking (+2.8 points), aligning with our earlier observation that random schedules accentuate early answer convergence. The improvement persists under more informed heuristics (low-confidence: +1.4; top-k margin: +0.7), indicating that Prophet's stopping rule complements, rather than replaces, token-selection policies.

6 CONCLUSION

In this work, we identified and leveraged a fundamental yet overlooked property of diffusion language models: early answer convergence. Our analysis revealed that up to 99% of instances can be correctly decoded using only half the refinement steps, challenging the necessity of conventional full-length decoding. Building on this observation, we introduced Prophet, a training-free early commit decoding paradigm that dynamically monitors confidence gaps to determine optimal termination points. Experiments on LLaDA-8B and Dream-7B demonstrate that Prophet achieves up to 3.4× reduction in decoding steps while maintaining generation quality. By recasting DLM decoding as an optimal stopping problem rather than a fixed-budget iteration, our work opens new avenues for efficient DLM inference and suggests that early convergence is a core characteristic of how these models internally resolve uncertainty, across diverse tasks and settings.

REFERENCES

Sudhanshu Agrawal, Risheek Garrepalli, Raghavv Goel, Mingu Lee, Christopher Lott, and Fatih Porikli. Spiffy: Multiplying diffusion llm acceleration via lossless speculative decoding, 2025. URL https://arxiv.org/abs/2509.18085.

Marianne Arriola, Aaron Gokaslan, Justin T. Chiu, Zhihan Yang, Zhixuan Qi, Jiaqi Han, Subham Sekhar Sahoo, and Volodymyr Kuleshov. Block diffusion: Interpolating between autoregressive and diffusion language models, 2025. URL https://arxiv.org/abs/2503.09573.

Jacob Austin, Daniel D Johnson, Jonathan Ho, Daniel Tarlow, and Rianne Van Den Berg. Structured denoising diffusion models in discrete state-spaces. *Advances in neural information processing systems*, 34:17981–17993, 2021a.

Jacob Austin, Augustus Odena, Maxwell Nye, Maarten Bosma, Henryk Michalewski, David Dohan, Ellen Jiang, Carrie Cai, Michael Terry, Quoc Le, et al. Program synthesis with large language models. *arXiv preprint arXiv:2108.07732*, 2021b.

Yonatan Bisk, Rowan Zellers, Jianfeng Gao, Yejin Choi, et al. Piqa: Reasoning about physical commonsense in natural language. In *Proceedings of the AAAI conference on artificial intelligence*, 2020.

Andrew Campbell, Joe Benton, Valentin De Bortoli, Thomas Rainforth, George Deligiannidis, and Arnaud Doucet. A continuous time framework for discrete denoising models. *Advances in Neural Information Processing Systems*, 35:28266–28279, 2022.

Mark Chen, Jerry Tworek, Heewoo Jun, Qiming Yuan, Henrique Ponde De Oliveira Pinto, Jared Kaplan, Harri Edwards, Yuri Burda, Nicholas Joseph, Greg Brockman, et al. Evaluating large language models trained on code. *arXiv preprint arXiv:2107.03374*, 2021.

Xinhua Chen, Sitao Huang, Cong Guo, Chiyue Wei, Yintao He, Jianyi Zhang, Hai Li, Yiran Chen, et al. Dpad: Efficient diffusion language models with suffix dropout. *arXiv preprint arXiv:2508.14148*, 2025.

Peter Clark, Isaac Cowhey, Oren Etzioni, Tushar Khot, Ashish Sabharwal, Carissa Schoenick, and Oyvind Tafjord. Think you have solved question answering? try arc, the ai2 reasoning challenge. *arXiv:1803.05457v1*, 2018.

Karl Cobbe, Vineet Kosaraju, Mohammad Bavarian, Mark Chen, Heewoo Jun, Lukasz Kaiser, Matthias Plappert, Jerry Tworek, Jacob Hilton, Reiichiro Nakano, et al. Training verifiers to solve math word problems. *arXiv preprint arXiv:2110.14168*, 2021.

Google DeepMind. Gemini-diffusion, 2025. URL https://blog.google/technology/google-deepmind/gemini-diffusion/.

Daniel T Gillespie. Approximate accelerated stochastic simulation of chemically reacting systems. *The Journal of chemical physics*, 115(4):1716–1733, 2001.

Shansan Gong, Shivam Agarwal, Yizhe Zhang, Jiacheng Ye, Lin Zheng, Mukai Li, Chenxin An, Peilin Zhao, Wei Bi, Jiawei Han, et al. Scaling diffusion language models via adaptation from autoregressive models. *arXiv preprint arXiv:2410.17891*, 2024.

Dan Hendrycks, Collin Burns, Saurav Kadavath, Akul Arora, Steven Basart, Eric Tang, Dawn Song, and Jacob Steinhardt. Measuring mathematical problem solving with the math dataset. *arXiv preprint arXiv:2103.03874*, 2021.

Jonathan Ho, Ajay Jain, and Pieter Abbeel. Denoising diffusion probabilistic models. *Advances in neural information processing systems*, 33:6840–6851, 2020.

Emiel Hoogeboom, Didrik Nielsen, Priyank Jaini, Patrick Forré, and Max Welling. Argmax flows and multinomial diffusion: Learning categorical distributions. *Advances in Neural Information Processing Systems*, 34:12454–12465, 2021.

Zhanqiu Hu, Jian Meng, Yash Akhauri, Mohamed S Abdelfattah, Jae-sun Seo, Zhiru Zhang, and Udit Gupta. Accelerating diffusion language model inference via efficient kv caching and guided diffusion. *arXiv preprint arXiv:2505.21467*, 2025.

Chihan Huang and Hao Tang. Ctrldiff: Boosting large diffusion language models with dynamic block prediction and controllable generation. *arXiv preprint arXiv:2505.14455*, 2025.

Daniel Israel, Guy Van den Broeck, and Aditya Grover. Accelerating diffusion llms via adaptive parallel decoding. *arXiv preprint arXiv:2506.00413*, 2025a.

Daniel Israel, Guy Van den Broeck, and Aditya Grover. Accelerating diffusion llms via adaptive parallel decoding, 2025b. URL https://arxiv.org/abs/2506.00413.

Bowen Jing, Gabriele Corso, Jeffrey Chang, Regina Barzilay, and Tommi Jaakkola. Torsional diffusion for molecular conformer generation. *Advances in neural information processing systems*, 35:24240–24253, 2022.

Inception Labs, Samar Khanna, Siddhant Kharbanda, Shufan Li, Harshit Varma, Eric Wang, Sawyer Birnbaum, Ziyang Luo, Yanis Miraoui, Akash Palrecha, Stefano Ermon, Aditya Grover, and Volodymyr Kuleshov. Mercury: Ultra-fast language models based on diffusion, 2025. URL https://arxiv.org/abs/2506.17298.

Stephanie Lin, Jacob Hilton, and Owain Evans. Truthfulqa: Measuring how models mimic human falsehoods. *arXiv preprint arXiv:2109.07958*, 2021.

Zhiyuan Liu, Yicun Yang, Yaojie Zhang, Junjie Chen, Chang Zou, Qingyuan Wei, Shaobo Wang, and Linfeng Zhang. dllm-cache: Accelerating diffusion large language models with adaptive caching. *arXiv preprint arXiv:2506.06295*, 2025a.

Zhiyuan Liu, Yicun Yang, Yaojie Zhang, Junjie Chen, Chang Zou, Qingyuan Wei, Shaobo Wang, and Linfeng Zhang. dllm-cache: Accelerating diffusion large language models with adaptive caching, 2025b. URL https://arxiv.org/abs/2506.06295.

Aaron Lou, Chenlin Meng, and Stefano Ermon. Discrete diffusion language modeling by estimating the ratios of the data distribution. *arXiv preprint arXiv:2310.16834*, 2023.

Xinyin Ma, Runpeng Yu, Gongfan Fang, and Xinchao Wang. dkv-cache: The cache for diffusion language models. *arXiv preprint arXiv:2505.15781*, 2025a.

Xinyin Ma, Runpeng Yu, Gongfan Fang, and Xinchao Wang. dkv-cache: The cache for diffusion language models, 2025b. URL https://arxiv.org/abs/2505.15781.

Alexander Quinn Nichol and Prafulla Dhariwal. Improved denoising diffusion probabilistic models. In *International conference on machine learning*, pp. 8162–8171. PMLR, 2021.

Shen Nie, Fengqi Zhu, Zebin You, Xiaolu Zhang, Jingyang Ou, Jun Hu, Jun Zhou, Yankai Lin, Ji-Rong Wen, and Chongxuan Li. Large language diffusion models. *arXiv preprint arXiv:2502.09992*, 2025.

Jingyang Ou, Shen Nie, Kaiwen Xue, Fengqi Zhu, Jiacheng Sun, Zhenguo Li, and Chongxuan Li. Your absorbing discrete diffusion secretly models the conditional distributions of clean data. *arXiv preprint arXiv:2406.03736*, 2024.

Aditya Ramesh, Mikhail Pavlov, Gabriel Goh, Scott Gray, Chelsea Voss, Alec Radford, Mark Chen, and Ilya Sutskever. Zero-shot text-to-image generation. In *International conference on machine learning*, pp. 8821–8831. Pmlr, 2021.

David Rein, Betty Li Hou, Asa Cooper Stickland, Jackson Petty, Richard Yuanzhe Pang, Julien Dirani, Julian Michael, and Samuel R Bowman. Gpqa: A graduate-level google-proof q&a benchmark. *arXiv preprint arXiv:2311.12022*, 2023.

Chitwan Saharia, Jonathan Ho, William Chan, Tim Salimans, David J Fleet, and Mohammad Norouzi. Image super-resolution via iterative refinement. *IEEE transactions on pattern analysis and machine intelligence*, 45(4):4713–4726, 2022.

Subham Sahoo, Marianne Arriola, Yair Schiff, Aaron Gokaslan, Edgar Marroquin, Justin Chiu, Alexander Rush, and Volodymyr Kuleshov. Simple and effective masked diffusion language models. *Advances in Neural Information Processing Systems*, 37:130136–130184, 2024.

Keisuke Sakaguchi, Ronan Le Bras, Chandra Bhagavatula, and Yejin Choi. Winogrande: An adversarial winograd schema challenge at scale. *Communications of the ACM*, 64(9):99–106, 2021.

Jiaxin Shi, Kehang Han, Zhe Wang, Arnaud Doucet, and Michalis K Titsias. Simplified and generalized masked diffusion for discrete data. *arXiv preprint arXiv:2406.04329*, 2024.

Jascha Sohl-Dickstein, Eric Weiss, Niru Maheswaranathan, and Surya Ganguli. Deep unsupervised learning using nonequilibrium thermodynamics. In *International conference on machine learning*, pp. 2256–2265. PMLR, 2015.

Yuerong Song, Xiaoran Liu, Ruixiao Li, Zhigeng Liu, Zengfeng Huang, Qipeng Guo, Ziwei He, and Xipeng Qiu. Sparse-dllm: Accelerating diffusion llms with dynamic cache eviction, 2025a. URL https://arxiv.org/abs/2508.02558.

Yuxuan Song, Zheng Zhang, Cheng Luo, Pengyang Gao, Fan Xia, Hao Luo, Zheng Li, Yuehang Yang, Hongli Yu, Xingwei Qu, Yuwei Fu, Jing Su, Ge Zhang, Wenhao Huang, Mingxuan Wang, Lin Yan, Xiaoying Jia, Jingjing Liu, Wei-Ying Ma, Ya-Qin Zhang, Yonghui Wu, and Hao Zhou. Seed diffusion: A large-scale diffusion language model with high-speed inference, 2025b. URL https://arxiv.org/abs/2508.02193.

Wen Wang, Bozhen Fang, Chenchen Jing, Yongliang Shen, Yangyi Shen, Qiuyu Wang, Hao Ouyang, Hao Chen, and Chunhua Shen. Time is a feature: Exploiting temporal dynamics in diffusion language models, 2025a. URL https://arxiv.org/abs/2508.09138.

Xu Wang, Chenkai Xu, Yijie Jin, Jiachun Jin, Hao Zhang, and Zhijie Deng. Diffusion llms can do faster-than-ar inference via discrete diffusion forcing, aug 2025b. URL https://arxiv.org/abs/2508.09192. arXiv:2508.09192.

Qingyan Wei, Yaojie Zhang, Zhiyuan Liu, Dongrui Liu, and Linfeng Zhang. Accelerating diffusion large language models with slowfast: The three golden principles. *arXiv preprint arXiv:2506.10848*, 2025a.

Qingyan Wei, Yaojie Zhang, Zhiyuan Liu, Dongrui Liu, and Linfeng Zhang. Accelerating diffusion large language models with slowfast sampling: The three golden principles, 2025b. URL https://arxiv.org/abs/2506.10848.

Chengyue Wu, Hao Zhang, Shuchen Xue, Zhijian Liu, Shizhe Diao, Ligeng Zhu, Ping Luo, Song Han, and Enze Xie. Fast-dllm: Training-free acceleration of diffusion llm by enabling kv cache and parallel decoding. *arXiv preprint arXiv:2505.22618*, 2025a.

Chengyue Wu, Hao Zhang, Shuchen Xue, Zhijian Liu, Shizhe Diao, Ligeng Zhu, Ping Luo, Song Han, and Enze Xie. Fast-dllm: Training-free acceleration of diffusion llm by enabling kv cache and parallel decoding, 2025b. URL https://arxiv.org/abs/2505.22618.

Jiacheng Ye, Zhihui Xie, Lin Zheng, Jiahui Gao, Zirui Wu, Xin Jiang, Zhenguo Li, and Lingpeng Kong. Dream 7b: Diffusion large language models. *arXiv preprint arXiv:2508.15487*, 2025.

Rowan Zellers, Ari Holtzman, Yonatan Bisk, Ali Farhadi, and Yejin Choi. Hellaswag: Can a machine really finish your sentence? *arXiv preprint arXiv:1905.07830*, 2019.

Kaiwen Zheng, Yongxin Chen, Hanzi Mao, Ming-Yu Liu, Jun Zhu, and Qinsheng Zhang. Masked diffusion models are secretly time-agnostic masked models and exploit inaccurate categorical sampling. *arXiv preprint arXiv:2409.02908*, 2024.

APPENDIX

A ADDITIONAL RESULTS

(a) MMLU w/o suffix prompt (low confidence)

(b) MMLU w/ suffix prompt (low confidence)

(c) MMLU w/o suffix prompt (random)

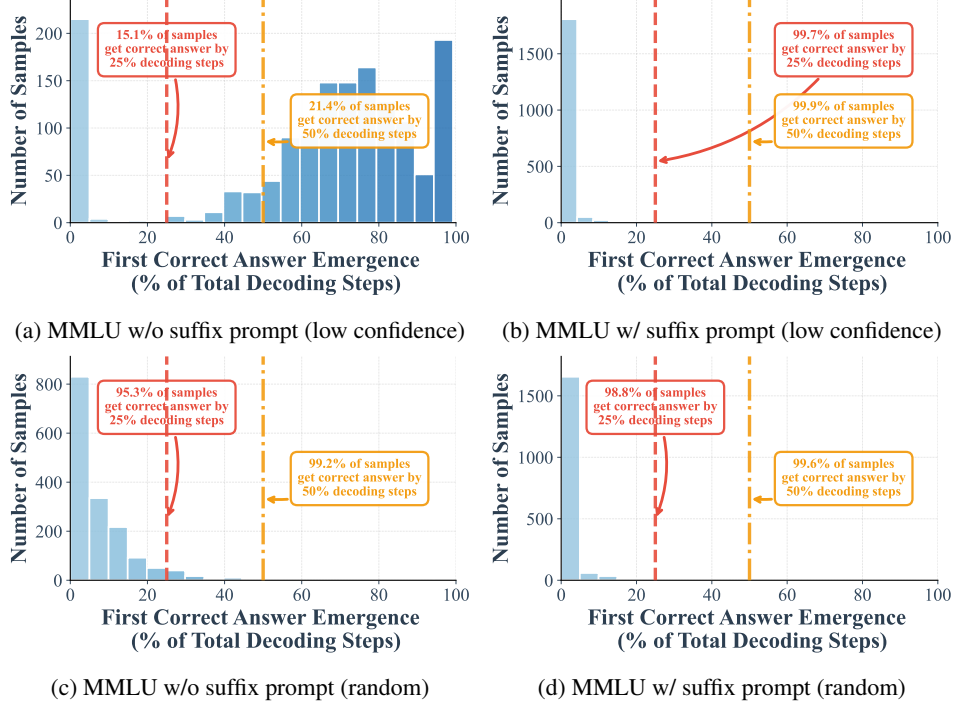(d) MMLU w/ suffix prompt (random)

Figure 4: **Distribution of early correct answer detection during decoding process.** Histograms show when correct answers first emerge during diffusion decoding, measured as percentage of total decoding steps, using `LLaDA 8B` on MMLU. Red and orange dashed lines indicate 50% and 70% completion thresholds, with corresponding statistics showing substantial early convergence. Suffix prompting (b,d) dramatically accelerates convergence compared to standard prompting (a,c). This early convergence pattern demonstrates that correct answer tokens stabilize as top-1 candidates well before full decoding.

Table 4: **Configurations used in our runs.** We keep only parameters relevant to our method: base budget (L, T, B) and PROPHET's confidence schedule.

Benchmark	Base Budget (L, T, B)	PROPHET Thresholds $(\tau_{\text{high}}, \tau_{\text{mid}}, \tau_{\text{low}})$	Transition Points
MMLU	L=64, T=64, B=16	(7.5, 5.0, 2.5)	33%, 67%
ARC-C	L=64, T=64, B=16	(7.5, 5.0, 2.5)	33%, 67%
Hellaswag	L=64, T=64, B=16	(7.5, 5.0, 2.5)	33%, 67%
TruthfulQA	L=64, T=64, B=16	(7.5, 5.0, 2.5)	33%, 67%
WinoGrande	L=64, T=64, B=16	(7.5, 5.0, 2.5)	33%, 67%
PIQA	L=64, T=64, B=16	(7.5, 5.0, 2.5)	33%, 67%
GSM8K	L=256, T=256, B=32	(8.0, 5.0, 3.5)	33%, 67%
GPQA	L=256, T=256, B=32	(8.0, 5.0, 3.5)	33%, 67%
HumanEval	L=512, T=512, B=32	(7.5, 5.0, 4.5)	33%, 67%
MBPP	L=512, T=512, B=32	(7.5, 5.0, 4.5)	33%, 67%
Sudoku	L=24, T=24, B=24	(7.5, 5.0, 2.5)	33%, 67%
Countdown	L=32, T=32, B=32	(7.5, 5.0, 2.5)	33%, 67%

B   EVALUATION DETAILS

We re-implemented the evaluation of LLADA and DREAM on those reported datasets. We generate and extract the final answer instead of comparing the log probability in the multiple-choice setting, which can lower the reported scores on some datasets because the model sometimes fails to produce an answer in the given format. The configuration of each experiment is summarized in Table 4.